Iranian Journal of Medical Physics

ijmp.mums.ac.ir

Brain Nucleus Changes in Cognitive Disorders: Examining By the Quantitative Susceptibility Mapping (QSM) Technique

Farzaneh Nikparast[1], Ali Shoeibi[3], Shabnam Niroumand[4], Hossein Akbari-Lalimi[1], Hoda Zare[1,2*]

1. Medical Physics Research Center, Mashhad University of Medical Sciences, Mashhad, Iran
2. Department of Medical Physics, Faculty of Medicine, Mashhad University of Medical Sciences, Mashhad, Iran
3. Department of Neurology, School of Medicine, Mashhad University of Medical Sciences, Mashhad, Iran
4. Department of Community Medicine, Faculty of Medicine, Mashhad University of Medical Sciences, Mashhad, Iran.

ARTICLE INFO

Article type:
Original Paper

Article history:
Received: Oct 15, 2022
Accepted: Dec 25, 2022

Keywords:
Quantitative Susceptibility Mapping
Alzheimer's Disease
Iron Deposition
Magnetic Susceptibility

ABSTRACT

Introduction: Iron deposition is vital for damaging neurons and causing different cognitive disorders. Today, using the quantitative susceptibility mapping (QSM) technique, iron deposits in other brain areas can be assessed and measured. This study aimed to identify changes in iron deposition of 12 brain nuclei through different stages of dementia using the QSM technique to introduce biomarkers for the early detection of cognitive disorders.

Material and Methods: The Alzheimer's Disease Neuroimaging Initiative (ADNI) database was used to download data. A 3T MRI scanner scanned thirty-five participants with normal cognition and forty-six patients with cognitive disorders who were classified into four groups based on the severity of the condition. QSM processing determined twelve regions of interest (ROIs) by automatic nuclei segmentation and statistical analysis performed in these groups' MRI images.

Results: Based on previous findings, QSM values increase proportionally to iron deposition. In this study, the increase in the QSM values of different nuclei of the early mild cognitive impairment (EMCI) stage indicates iron deposition in these participants. In the EMCI group, The QSM value of the bilateral thalamus ($P<0.05$) and left amygdala ($P=0.006$) nuclei were higher than ***in*** the control group. Based on the results of the receiver operating characteristic curve (ROC) analysis, the left amygdala ($P=0.005$), left putamen ($P=0.002$), left thalamus ($P=0.05$), and right thalamus ($P<0.05$) have an appropriate sensitivity and specificity to identify the different stages of cognitive disorders.

Conclusion: The left amygdala and bilateral thalamic nuclei are the first areas exposed to iron deposition during cognitive impairment. Mentioned nuclei, especially the left amygdala, have high efficiency and sensitivity for the early detection of cognitive disorders.

► *Please cite this article as:*
Nikparast F, Shoeibi A, Niroumand Sh, Akbari-Lalimi H, Zare H. Brain Nucleus Changes in Cognitive Disorders: Examining By the Quantitative Susceptibility Mapping (QSM) Technique. Iran J Med Phys 2024; 21: 45-52. 10.22038/IJMP.2022.68457.2198.

Introduction

Neurodegenerative Alzheimer's disease (AD), more common in the elderly, imposes a heavy economic, psychological, and social burden on individuals and society [1, 2].

There are usually stages of dementia that have an increased risk of developing AD compared to healthy people, which include subjective memory concerns (SMC), early mild cognitive impairment (EMCI), and late mild cognitive impairment (LMCI), respectively [3].

Various changes in the brain lead to the development and progression of these disorders; pathological changes usually occur earlier than morphological changes [4, 5]; Iron deposition and amyloid-beta plaque aggregations are among the most important pathological changes in the brain during AD [6, 7].

Iron is the most abundant paramagnetic substance in the body, playing a pivotal role in performing many biological activities, such as cell division and gene expression; it is stored in the brain as ferritin or hemosiderin-6 forms and causes positive changes in the magnetic susceptibility of the tissue [8].

Despite all the benefits of iron, excessive deposition in different brain areas can damage neurons and impair cognitive function [9]; areas of increased iron deposition are prone to the accumulation of amyloid-beta plaques, one of the most well-known marks of AD [10].

According to various studies, there is a clear link between iron deposition and the development of neurodegenerative disorders such as AD and Parkinson's disease, so early detection of these iron and amyloid-beta plaque deposits leads to diagnosing these diseases in the early stages [11].

One of the most popular imaging modalities for brain sediment detection is positron emission tomography (PET); however, high ionizing radiation levels limit its safe clinical use [12].

*Corresponding Author: Tel: +98-5138002321; Fax: +98-5138002320; Email: zareh@mums.ac.ir

There are various magnetic resonance imaging (MRI)-based techniques to identify these iron deposition areas, such as $T2^*$ weighted imaging ($T2^*$ WI), susceptibility-weighted imaging (SWI), transverse relaxation rate ($R2^*$), field-dependent relaxation rate increase (FDRI), and calculation of Susceptibility through multiple orientation sampling (COSMOS).

Besides their benefits, each technique has several disadvantages; for example, most methods mentioned above suffer from Blooming artifact [13]; T2* WI depends on the scan parameters; the SWI method depends on the patient's head position and the magnetic susceptibility of the tissues around the target area [14].

Also, the values obtained from the $R2^*$ technique depend on the iron and water content of the tissue; to perform the FDRI technique, we need two magnetic fields with two different strengths, and finally, in the COSMOS technique, the patient's head should be scanned in different directions [15-20].

These limitations complicate the widespread use of these methods in the clinical field.

One of the essential features of body tissues is their magnetic susceptibility, an inherent characteristic of body tissues in response to the application of external magnetic fields and express tissue constituents.

The presence of diamagnetic substances in the brain, such as calcium and white matter, reduces magnetic susceptibility, and paramagnetic substances, such as iron, increase the tissue's magnetic susceptibility [21].

Recently, a technique based on changes in magnetic susceptibility, called quantitative susceptibility mapping (QSM), which can apply to many routine MRI sequences, has been introduced [16, 22].

This technique involves post-processing algorithms applied to the phase and magnitude images with different MRI sequences; It creates a map in part-per-million (ppm) indicating the areas increased or decreased in terms of changes in magnetic susceptibility [23-25].

So far, various types of research have been done using this technique to evaluate neurodegenerative diseases [11, 26-28]. This research project aims to identify the first brain nuclei pathological changes in the spectrum of cognitive disorders, which leads to introducing a suitable biomarker for the early detection of cognitive impairment.

Materials and Methods

Database

Data were obtained from the Alzheimer's Disease Neuroimaging Initiative (ADNI) database. The ADNI was launched in 2003 as a public-private partnership by Principal Investigator Michael W. Weiner, MD. The primary goal of ADNI has been to test whether serial MRI, positron emission tomography (PET), other biological markers, and clinical and neuropsychological assessment can be combined to measure the progression of mild cognitive impairment MCI and early AD.

The ADNI3 project was launched in 2016 to determine the relationships between clinical, cognitive, imaging, genetic, and biochemical biomarkers across the spectrum of AD.

Scientists of this institution are working on 59 research centers in the United States and Canada. This project aims to identify the pathological changes in the brain that trigger these disorders.

Participants

Based on the data, thirty-five cognitively normal and forty-six participants with cognitive impairment disorders were included in this study. We classified the cognitive disorders group into four groups based on cognitive test scores and assessments performed by ADNI specialists.

Inclusion criteria for subject selection include:

1. People should be in one of the five groups: cognitively normal (CN), subjective memory concerns (SMC), Early mild cognitive impairment (EMCI), late mild cognitive impairment (LMCI), and AD (Alzheimer's disease).
2. Multi-echo GRE and T1W scans of these people should be available.
3. Phase and magnitude images should be available separately.
   Each GRE multi-echo image contains two real and imaginary parts.
   The real part creates the magnitude image, and the imaginary part makes the phase image for us; we need to use both images in this research.
4. Information about cognitive information, such as MMSE scores, should be available.

The participants' demographic characteristics are given in Table 1.

MRI Acquisition

All patients' MRI scans were performed using the Siemens Prisma 3.0T MRI scanner equipped with a Head-Neck coil.

For a Brain MRI scan, the patient should lie in a supine position, and the center of the sternum must be aligned with the center of the spine coil.

3D Accelerated_Sagittal_MPRAGE sequence was performed with the following parameters: TR (ms) =2300, TE/TI (ms) =2.98/900, Slice Thickness (mm) =1, Flip Angle=9, Pixel Bandwidth=240, and Acquisition Matrix and Reconstruction Matrix=240.

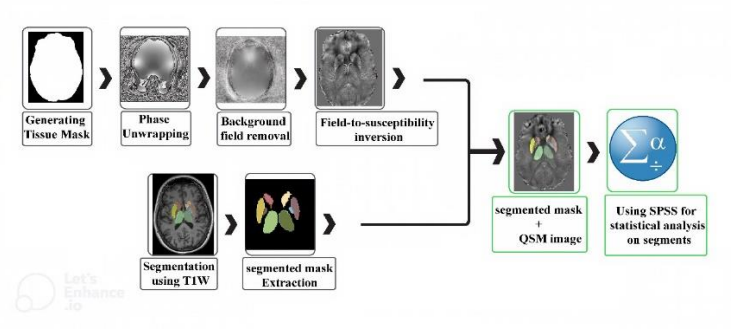

Figure1. QSM reconstruction steps

GRE multi-echo sequence was performed with three different times of echoes (3TE) with the following parameters: TR (ms) =650, TE1-TE2-TE3 (ms) =6.09-13-20**,** Slice Thickness (mm) =4, Flip Angle=20, Pixel Bandwidth=260, Matrix size=256×256, Voxel size x (mm) = 0.859375, Voxel size y (mm) =0.859375 and Number of slices=44.

Image Processing

Quantitative Susceptibility Mapping

QSM reconstruction has four steps: generating tissue mask, phase unwrapping, background field removal, and field-to-susceptibility inversion (Figure 1). Each step is performed with different algorithms and toolboxes [23].

After making QSM images, it is time to segment and determine the region of interest (ROIs) to evaluate the QSM values of each area in terms of ppm. The basis of this reconstruction is done on the brain tissue, so first, we need to separate the brain tissue from the skull bone in the magnitude image. This brain tissue extraction was performed using the Brain Extraction Tool from the FMRIB Software Library [29].

In the next step, to prevent the occurrence of the aliasing artifact in the phase images and total QSM reconstruction, we performed the phase unwrapping using a Laplacian-based phase unwrapping tool from STI Suite, the MATLAB toolbox[30].

Phase removal was done using the V-SHARP tool from the STI suite MATLAB toolbox to eliminate the unwanted consequences of the border areas, QSM reconstruction, or the susceptibility map was computed by the streaking artifacts reduction (STAR) algorithm [31, 32].

For the accuracy of the between-group analysis, a reference was made to the brain mask during QSM reconstruction [33];The SEPIA toolbox was used to perform the above steps [34].

Automatic Segmentation

To create the region of interest (ROIs) mask, we performed automatic segmentation using the FMRIB Software Library, a model-based segmentation/registration tool[35].

At this stage, the location of twelve nuclei was determined, including left-thalamus, left-caudate, left-putamen, left-pallidum, left-hippocampus, left-amygdala, right-thalamus, right-caudate, right-putamen, right-pallidum, right-hippocampus, and right-amygdala.

A neurologist confirmed the accuracy of these segments. In this step, we measured the magnetic susceptibility values of each nucleus using 3D Slicer software[36].

For each participant, the segmented mask and QSM image were defined as input for the software, and based on the FSL guide, we specified the nuclei name of each segment. Finally, we saved the mean magnetic susceptibility value for further statistical analysis from the calculated statistical parameters for each nucleus.

Statistical analysis

Statistical analyses were performed with the help of IBM Statistic SPSS (Statistical Package for Social Science) software V26. Comparing the age and MMSE scores variables among the groups was done using a one-way analysis of variance (ANOVA).

The chi-squared test was used for the same purpose as the qualitative gender variable.

After examining the normal distribution of data with the Kolmogorov-Smirnov test, ANOVA with post hoc test (Tukey-Kramer test) was used to assess the significant difference between the mean magnetic susceptibility of brain nuclei in 5 groups for normality values. Kruskal–Wallis and Mann–Whitney tests were also performed for non-normality values for the same purpose.

Finally, ROC curve analysis was performed on the brain nuclei of participants in all five groups. $P \leq 0.05$ was considered statistically significant in all statistical tests.

Results

Participants characteristics

Based on the results, the age variable did not differ significantly between the study groups, while there was a significant difference between MMSE scores among the target groups.

MMSE scores were significantly different between AD groups and SMC (P <0.001), AD and EMCI (P <0.001), AD and control (P <0.001), SMCI and LMCI (P =0.025), and LMCI compared to control (P =0.002).

Also, a significant difference was observed between the number of men and women in the study groups (P=0.04); the analyzed demographic information can be seen in Table 1.

Table 1. The results of the participant's demographic analysis. (Chi-squared and ANOVA analysis.)

Characteristic	CN (35)	SMC (10)	EMCI (17)	LMCI (9)	AD (10)	P-Value
Age (Mean±SD)	73.34±8.07	77.7±3.65	76.76±6.28	77.44±5.15	78.7±6.83	P=0.11
MMSE Score (Mean±SD)	29.0±1.43	28.80±1.13	27.35±1.96	24.6667±6.81	21.75±4.30	P < 0.001
Sex	23Female and 12 Male	7 Female and 3 Male	4 Female and 13 Male	4 Female and 5 Male	5 Female and 5 Male	P=0.04

CN, cognitively normal; SMC, subjective memory concerns; EMCI, early mild cognitive impairment; LMCI, late mild cognitive impairment; AD, Alzheimer's disease; MMSE, Mini-Mental State Examination. P ≤ 0.05 was considered statistically significant, and bold font indicates statistical significance.

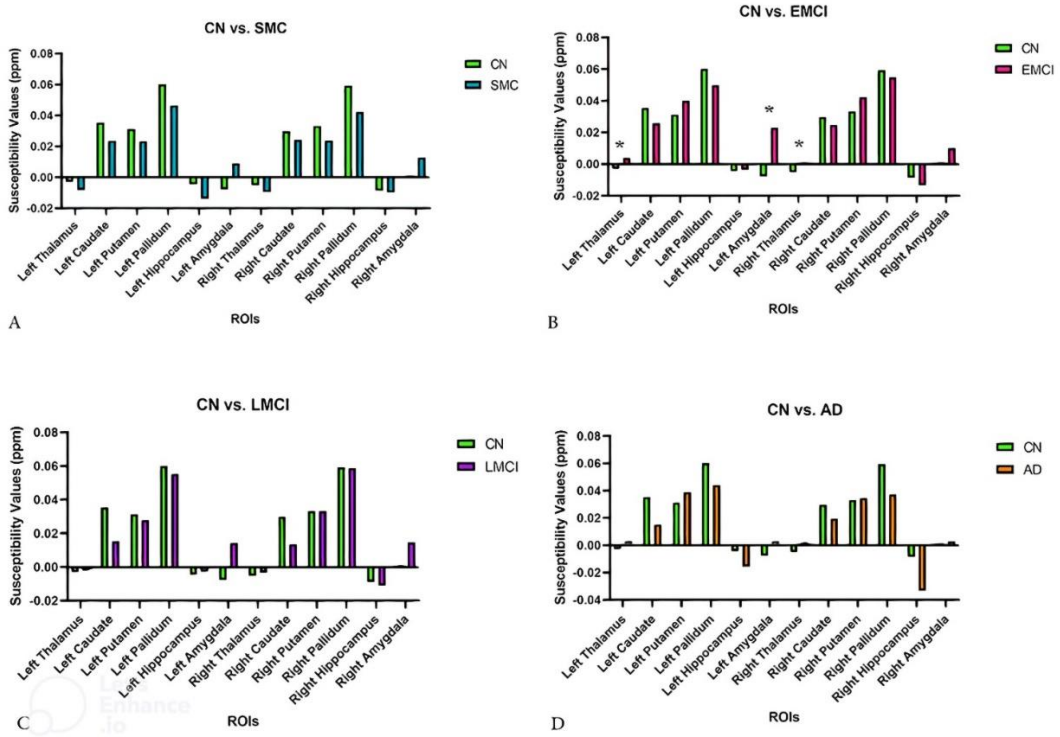

Figure 2. Mean susceptibility values of brain nuclei of patients with SMC (A), EMCI (B), LMCI (C), and AD (D) compared to the cognitively normal group

Table 2. Comparison of brain nuclei QSM values between study groups using one-way analysis of variance

One Way ANOVA							
		group					
		AD	SMCI	EMCI	LMCI	control	P-Value
Left Thalamus	Mean	.0031	-.0083	.0035	-.0020	-.0045	0.004*
	Std. Deviation	.01086	.01034	.01116	.00875	.00829	
Left Caudate	Mean	.0152	.0236	.0249	.0154	.0377	0.037*
	Std. Deviation	.01871	.01765	.03994	.02255	.02373	
Left Putamen	Mean	.0390	.0234	.0411	.0279	.0220	0.066
	Std. Deviation	.03391	.01564	.02076	.02006	.02257	
Right Thalamus	Mean	.0023	-.0095	.0013	-.0033	-.0074	0.008*
	Std. Deviation	.01264	.01262	.00934	.01028	.00879	
Right Caudate	Mean	.0196	.0242	.0257	.0135	.0293	0.291
	Std. Deviation	.02175	.01804	.02953	.01981	.02154	
Right Putamen	Mean	.0346	.0237	.0442	.0331	.0243	0.208
	Std. Deviation	.03388	.01983	.03104	.02128	.02194	
Right Pallidum	Mean	.0374	.0423	.0528	.0587	.0564	0.132
	Std. Deviation	.03428	.03129	.01857	.02710	.02128	
Right Hippocampus	Mean	-.0333	-.0097	-.0148	-.0108	-.0082	0.224
	Std. Deviation	.04090	.02633	.03601	.03147	.02352	

*p ≤ 0.05 was considered statistically significant, and bold font indicates statistical significance

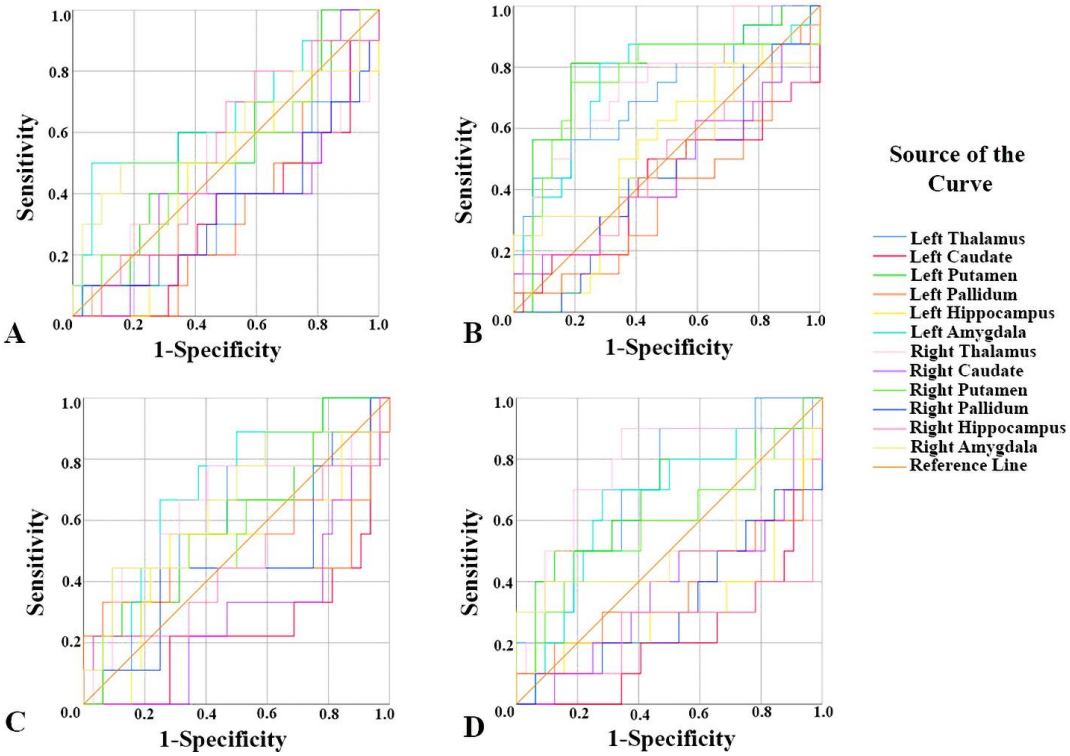

Figure3. Results of ROC curve analysis of QSM values obtained from the twelve region-of-interests to differentiate SMC (A), EMCI (B), LMCI (C), and AD (D) subjects from the cognitively normal group.

Evaluation of regional susceptibility

Based on the results of the analysis, QSM values in the EMCI group significantly increased in the left thalamus (P =0.021), left amygdala (P =0.006), and right thalamus (P =0.049) compared to the CN group (Figure 2, Table 2, Supplementary Table 3, Supplementary Table 4).

ROC curve analysis

None of the nuclei had the sensitivity and specificity to diagnose SMC patients from the CN group (Supplementary Table 5).

In the EMCI group, Area Under the Curve (AUC) values in the left thalamus (P=0.017), left putamen (P=0.002), right thalamus (P=0.006), left amygdala (P=0.005), and right putamen (P=0.005) were over 0.7 (Supplementary Table 6).

The highest sensitivity belongs to the left amygdala and left putamen nuclei, with 81% in this group.

In the LMCI group, only the left amygdala nucleus with an AUC value greater than 0.7 (P = 0.047) is effective in diagnosing LMCI patients; the sensitivity of this variable is 66%, and its specificity is 75% (Supplementary Table 7).

In the AD group, the highest AUC values were obtained in the left and right thalamic nuclei, which are 0.7 (P=0.050) and 0.76 (P=0.011), respectively.

These two nuclei also have the highest sensitivity in identifying AD patients based on QSM values (Supplementary Table 8) (Figure 3).

Discussion

Iron deposition and amyloid-beta plaques in the deep nuclei of the brain represent microscopic or pathological changes that occur before the appearance of morphological changes such as atrophy of different brain areas; However, because of the lack of reliable and sensitive biomarkers for these pathological changes, diagnosis is usually made based on clinical findings in the advanced stages of the disease.

The presence of these materials in the tissue causes changes in the QSM image; They create an excellent contrast if placed together.

Despite all the benefits of iron in the body, previous studies have shown that its deposition is closely related to various neurodegenerative diseases such as Alzheimer's and Parkinson's. Also, its presence has been proven as one of the main components of aging plaques and Neurofibrillary tangles (NFTs).

Excessive levels of iron stored in the brain produce toxic free radicals, oxidative damage, inflammation, and nervous system destruction.

According to Ayton et al.'s study, there is a strong correlation between iron accumulation in the inferior temporal gyrus (ITG) and cognitive decline in individuals with Aβ plaques, tau protein, and neurofibrillary tangles; The increasing iron concentration provides ideal conditions for the accumulation of amyloid beta and the occurrence of neurotoxicity [37].

Investigating the pattern of brain iron deposition during the stages of cognitive disorders leads to a better understanding of the pathophysiological process of the disease, introducing a reliable biomarker for early diagnosis of the disorder and, ultimately, a basis for targeted treatment.

Despite all the efforts made in this field, until now, the cause-and-effect relationship between iron accumulation and neurological diseases is unclear; however, monitoring the spatial and temporal distribution and the quantity of iron deposition leads to a better understanding of the progress of cognitive disorders and examining the sequence of pathological events.

This research project was implemented to achieve several goals.

It was initially, identifying the brain nucleus that undergoes the first changes in magnetic susceptibility in the early stages of cognitive disorders to introduce biomarkers for early detection of these stages.

Finally, the efficiency, sensitivity, and specificity of the QSM technique in diagnosing each group of patients were evaluated using the ROC curve.

Evaluation of regional susceptibility

Based on the results of previous research projects, the formation of primary amyloid-beta plaques is closely related to iron accumulation and the increase in iron deposits with the production of more amyloid-beta peptides [4, 38, 39].

Microscopic changes often lead to changes in the tissue's intrinsic properties and magnetic susceptibility.

Since the increase in QSM values is strongly proportional to the rise in iron deposition, biomarkers can be introduced to identify these disorders early [40] [41].

In the present study, a notable increase in QSM values of the left amygdala, right thalamus, and left thalamus of the EMCI group was observed compared to the control group, indicating the onset of pathological changes leading to neuronal activity damage at the beginning of cognitive impairment.

This increase in QSM values is also present in the nuclei of the left amygdala, right thalamus, and left thalamus of patients with AD, but there is no statistically significant difference.

The occurrence of the plateau effect may explain the reason for this effect in the AD group [42]. Also, a study conducted in 2019 by Mousa Zidan et al. to assess brain volume in MCI and AD patients found that a decrease in thalamic volume could be an early sign of poorer cognitive function in aMCI [43].

These findings align with previous studies' results in different study groups [44-46].

ROC curve analysis

This section aims to assess the efficiency, sensitivity, and specificity of the QSM technique as a new and non-invasive method in diagnosing patients with a range of cognitive disorders.

Initially, this technique was used to distinguish the SMC group, which was measured using the ROC curve.

Despite the relatively good sensitivity and specificity of some brain nuclei, none of the nuclei is suitable for differentiating SMC patients from healthy individuals because of the low level of AUC.

In the EMCI group, the left putamen and left amygdala nuclei are efficient and sensitive for diagnosing EMCI patients; in 81% of cases, people with this disease can be correctly interpreted by referring to the QSM values of these brain nuclei [45, 47].

In the LMCI group, only the left amygdala nucleus with efficiency, sensitivity, and specificity can diagnose these patients, which aligns with Kim's research results [45].

Finally, using this method in the AD group was evaluated using the ROC curve.

In this group, the right and left thalamus nuclei have the efficiency, sensitivity, and specificity to differentiate AD patients from healthy individuals, which aligns with Kim and Li's research results [45, 47].

Conclusion

The left amygdala nuclei, right thalamus, and left thalamus are the first areas exposed to iron deposition at the onset of cognitive impairment.

Because of the high efficiency, sensitivity, and specificity of QSM values of these nuclei, especially the left amygdala, they can be used as biomarkers for the early detection of cognitive disorders.

The QSM technique for diagnosing and monitoring a range of cognitive impairments is ideal.

Acknowledgment

The authors would like to express their gratitude to Mashhad University of Medical Sciences for the financial support of this thesis, with the following code of ethics: IR.MUMS.MEDICAL.REC.1400.510. The online version of the approval is available at the following address and is open to the public: https://ethics.research.ac.ir/IR.MUMS.MEDICAL.REC.1400.510

References

1. Sosa-Ortiz AL, Acosta-Castillo I, Prince MJ. Epidemiology of dementias and Alzheimer′s disease. Archives of medical research. 2012;43(8):600-8.
2. Mayeux R, Stern Y. Epidemiology of Alzheimer′s disease. Cold Spring Harbor perspectives in medicine. 2012;2(8):a006239.
3. Kazemi Y, Houghten S, editors. A deep learning pipeline to classify different stages of Alzheimer′s disease from fMRI data. 2018 IEEE Conference on Computational Intelligence in Bioinformatics and Computational Biology (CIBCB). 2018.
4. Gong NJ, Chan CC, Leung LM, Wong CS, Dibb R, Liu C. Differential microstructural and morphological abnormalities in mild cognitive

impairment and a lzheimer′s disease: Evidence from cortical and deep gray matter. Human brain mapping. 2017;38(5):2495-508.
5. Gong N-J, Kuzminski S, Clark M, Fraser M, Sundman M, Guskiewicz K, et al. Microstructural alterations of cortical and deep gray matter over a season of high school football revealed by diffusion kurtosis imaging. Neurobiology of disease. 2018;119:79-87.
6. van Bergen JMG, Li X, Quevenco FC, Gietl AF, Treyer V, Meyer R, et al. Simultaneous quantitative susceptibility mapping and Flutemetamol-PET suggests local correlation of iron and β-amyloid as an indicator of cognitive performance at high age. NeuroImage. 2018;174:308-16.
7. Liu J-L, Fan Y-G, Yang Z-S, Wang Z-Y, Guo C. Iron and Alzheimer′s Disease: From Pathogenesis to Therapeutic Implications. Frontiers in neuroscience. 2018;12:632-.
8. Bilgic B, Pfefferbaum A, Rohlfing T, Sullivan EV, Adalsteinsson E. MRI estimates of brain iron concentration in normal aging using quantitative susceptibility mapping. NeuroImage. 2012;59(3):2625-35.
9. Bolt H, Marchan R. Iron dysregulation: an important aspect in toxicology. Archives of toxicology. 2010;84(11):823-4.
10. Lee J-H, Lee M-S. Brain Iron Accumulation in Atypical Parkinsonian Syndromes: in vivo MRI Evidences for Distinctive Patterns. Frontiers in Neurology. 2019;10.
11. Syam K. Quantitative estimation of regional brain iron deposition-a potential biomarker for Parkinson′s Disease and other neurodegenerative conditions causing a typical Parkinsonism. SCTIMST; 2021.
12. Zhao Y, Raichle ME, Wen J, Benzinger TL, Fagan AM, Hassenstab J, et al. In vivo detection of microstructural correlates of brain pathology in preclinical and early Alzheimer Disease with magnetic resonance imaging. NeuroImage. 2017;148:296-304.
13. Li J, Chang S, Liu T, Wang Q, Cui D, Chen X, et al. Reducing the object orientation dependence of susceptibility effects in gradient echo MRI through quantitative susceptibility mapping. Magnetic resonance in medicine. 2012;68(5):1563-9.
14. Walsh AJ, Wilman AH. Susceptibility phase imaging with comparison to R2 mapping of iron-rich deep grey matter. NeuroImage. 2011;57(2):452-61.
15. Du L, Zhao Z, Cui A, Zhu Y, Zhang L, Liu J, et al. Increased Iron Deposition on Brain Quantitative Susceptibility Mapping Correlates with Decreased Cognitive Function in Alzheimer′s Disease. ACS chemical neuroscience. 2018;9(7):1849-57.
16. Langkammer C, Schweser F, Krebs N, Deistung A, Goessler W, Scheurer E, et al. Quantitative susceptibility mapping (QSM) as a means to measure brain iron? A post mortem validation study. NeuroImage. 2012;62(3):1593-9.
17. Li J, Chang S, Liu T, Wang Q, Cui D, Chen X, et al. Reducing the object orientation dependence of susceptibility effects in gradient echo MRI through quantitative susceptibility mapping. Magnetic resonance in medicine. 2012;68(5):1563-9.
18. Meadowcroft MD, Connor JR, Smith MB, Yang QX. MRI and histological analysis of beta-amyloid plaques in both human Alzheimer′s disease and APP/PS1 transgenic mice. Journal of Magnetic Resonance Imaging: An Official Journal of the International Society for Magnetic Resonance in Medicine. 2009;29(5):997-1007.
19. Wang Y, Liu T. Quantitative susceptibility mapping (QSM): decoding MRI data for a tissue magnetic biomarker. Magnetic resonance in medicine. 2015;73(1):82-101.
20. Liu T, Spincemaille P, De Rochefort L, Kressler B, Wang Y. Calculation of susceptibility through multiple orientation sampling (COSMOS): a method for conditioning the inverse problem from measured magnetic field map to susceptibility source image in MRI. Magnetic Resonance in Medicine: An Official Journal of the International Society for Magnetic Resonance in Medicine. 2009;61(1):196-204.
21. Hagemeier J, Zivadinov R, Dwyer MG, Polak P, Bergsland N, Weinstock-Guttman B, et al. Changes of deep gray matter magnetic susceptibitwoity over 2 years in multiple sclerosis and healthy control brain. NeuroImage Clinical. 2018;18:1007-16.
22. Cogswell PM, Wiste HJ, Senjem ML, Gunter JL, Weigand SD, Schwarz CG, et al. Associations of quantitative susceptibility mapping with Alzheimer′s disease clinical and imaging markers. NeuroImage. 2021;224:117433.
23. 23. Reichenbach J, Schweser F, Serres B, Deistung A. Quantitative susceptibility mapping: concepts and applications. Clinical neuroradiology. 2015;25(2):225-30.
24. Wen Y, Wang Y, Liu T. Enhancing k-space quantitative susceptibility mapping by enforcing consistency on the cone data (CCD) with structural priors. Magnetic resonance in medicine. 2016;75(2):823-30.
25. Sun H, Wilman AH. Background field removal using spherical mean value filtering and Tikhonov regularization. Magnetic resonance in medicine. 2014;71(3):1151-7.
26. Au CKF, Abrigo J, Liu C, Liu W, Lee J, Au LWC, et al. Quantitative Susceptibility Mapping of the Hippocampal Fimbria in Alzheimer′s Disease. Journal of Magnetic Resonance Imaging. 2021;53(6):1823-32.
27. Nikparast F, Ganji Z, Danesh Doust M, Faraji R, Zare H. Brain pathological changes during neurodegenerative diseases and their identification methods: How does QSM perform in detecting this process? Insights into Imaging. 2022;13(1):74.
28. Nikparast F, Ganji Z, Zare H. Early differentiation of neurodegenerative diseases using the novel QSM technique: what is the biomarker of each disorder? BMC Neurosci. 2022;23(1):48.
29. Straub S, Schneider TM, Emmerich J, Freitag MT, Ziener CH, Schlemmer HP, et al. Suitable reference tissues for quantitative susceptibility mapping of the brain. Magnetic resonance in medicine. 2017;78(1):204-14.
30. Li W, Wu B, Liu C. Quantitative susceptibility mapping of human brain reflects spatial variation in tissue composition. NeuroImage. 2011;55(4):1645-56.

31. Wei H, Dibb R, Zhou Y, Sun Y, Xu J, Wang N, et al. Streaking artifact reduction for quantitative susceptibility mapping of sources with large dynamic range. NMR in biomedicine. 2015;28(10):1294-303.
32. Li W, Wu B, Batrachenko A, Bancroft-Wu V, Morey RA, Shashi V, et al. Differential developmental trajectories of magnetic susceptibility in human brain gray and white matter over the lifespan. Human brain mapping. 2014;35(6):2698-713.
33. Feng X, Deistung A, Reichenbach JR. Quantitative susceptibility mapping (QSM) and R2* in the human brain at 3 T: Evaluation of intra-scanner repeatability. Zeitschrift für Medizinische Physik. 2018;28(1):36-48.
34. Chan K-S, Marques JP. SEPIA—susceptibility mapping pipeline tool for phase images. NeuroImage. 2021;227:117611.
35. Patenaude B, Smith SM, Kennedy DN, Jenkinson M. A Bayesian model of shape and appearance for subcortical brain segmentation. NeuroImage. 2011;56(3):907-22.
36. 36. Fedorov A, Beichel R, Kalpathy-Cramer J, Finet J, Fillion-Robin J-C, Pujol S, et al. 3D Slicer as an image computing platform for the Quantitative Imaging Network. Magnetic resonance imaging. 2012;30(9):1323-41.
37. Ayton S, Wang Y, Diouf I, Schneider JA, Brockman J, Morris MC, et al. Brain iron is associated with accelerated cognitive decline in people with Alzheimer pathology. Molecular psychiatry. 2020;25(11):2932-41.
38. Galante D, Cavallo E, Perico A, D′Arrigo C. Effect of ferric citrate on amyloid-beta peptides behavior. Biopolymers. 2018;109(6):e23224.
39. Tahmasebinia F, Emadi S. Effect of metal chelators on the aggregation of beta-amyloid peptides in the presence of copper and iron. Biometals. 2017;30(2):285-93.
40. Hwang EJ, Kim HG, Kim D, Rhee HY, Ryu CW, Liu T, et al. Texture analyses of quantitative susceptibility maps to differentiate Alzheimer′s disease from cognitive normal and mild cognitive impairment. Medical physics. 2016;43(8):4718.
41. Tiepolt S, Schäfer A, Rullmann M, Roggenhofer E, Gertz HJ, Schroeter ML, et al. Quantitative Susceptibility Mapping of Amyloid-β Aggregates in Alzheimer′s Disease with 7T MR. Journal of Alzheimer′s disease : JAD. 2018;64(2):393-404.
42. Peters DG, Connor JR, Meadowcroft MD. The relationship between iron dyshomeostasis and amyloidogenesis in Alzheimer′s disease: two sides of the same coin. Neurobiology of disease. 2015;81:49-65.
43. Zidan M, Boban J, Bjelan M, Todorović A, Stankov Vujanić T, Semnic M, et al. Thalamic volume loss as an early sign of amnestic mild cognitive impairment. Journal of Clinical Neuroscience. 2019;68:168-73.
44. Acosta-Cabronero J, Williams GB, Cardenas-Blanco A, Arnold RJ, Lupson V, Nestor PJ. In vivo quantitative susceptibility mapping (QSM) in Alzheimer′s disease. PloS one. 2013;8(11):e81093.
45. Kim HG, Park S, Rhee HY, Lee KM, Ryu CW, Rhee SJ, et al. Quantitative susceptibility mapping to evaluate the early stage of Alzheimer′s disease. NeuroImage Clinical. 2017;16:429-38.
46. Kan H, Uchida Y, Arai N, Ueki Y, Aoki T, Kasai H, et al. Simultaneous voxel-based magnetic susceptibility and morphometry analysis using magnetization-prepared spoiled turbo multiple gradient echo. NMR in biomedicine. 2020;33(5):e4272.
47. Li D, Liu Y, Zeng X, Xiong Z, Yao Y, Liang D, et al. Quantitative Study of the Changes in Cerebral Blood Flow and Iron Deposition During Progression of Alzheimer′s Disease. Journal of Alzheimer′s disease : JAD. 2020;78(1):439-52.